

Mixed mode crack propagation in cold drawn tubes subjected to torsional fatigue

S. Beretta¹, A. Cerrini¹ and H. Desimone²

¹ Politecnico di Milano, Mechanical Department, Via La Masa 34, 20158 Milano, Italy.

Corresponding author: stefano.beretta@polimi.

² Tenaris Dalmine, Piazza Caduti 1, 24044 Dalmine, Italy.

ABSTRACT

In a previous work by the authors, the torsional fatigue of micronotched - cold drawn tubes had been analyzed. Specimens with longitudinal shallow notches showed a dominant mode III propagation (throughout the tube thickness) even if mode I (at the defect edges) was present. Indeed, mode II crack propagation along the tube axis was observed in the second propagation stage.

In this work, the reason for this peculiar fatigue crack propagation is further investigated. In particular, the relationship between some 'equivalent' stress intensity factors proposed in the literature and crack growth rates is analysed. With this aim, alternating torsional crack propagation tests have been carried out on notched tubular specimens, being the trough-thickness notches both in longitudinal and transverse direction, in order to analyse the possible influence of the material anisotropy.

Mixed mode and pure mode II crack paths have been observed. The crack paths were analysed through FE analysis and the relationship between actual stress intensity factor and growth rates is discussed.

INTRODUCTION

In a previous work by the authors [1], the torsional fatigue of cold drawn tubes containing shallow longitudinal notches had been analysed. As shown in Fig. 1, the failure process was characterized by the growth (or threshold at the fatigue limit) of mode III fatigue cracks along the tube thickness and mode I at the defect edges, with a final mode II fatigue crack propagation in longitudinal direction.

In order to understand this kind of peculiar failure mechanism and to check the influence of micro structure due to the cold drawn process on crack growth rates and crack path, alternating torsion tests were performed on specimens extracted from a cold drawn tube in which a transevrsl or a longitudinal micro-notch has been artificially made. The experimental crack path has been modelled with FE for determining SIF's at different stages of crack propagation.

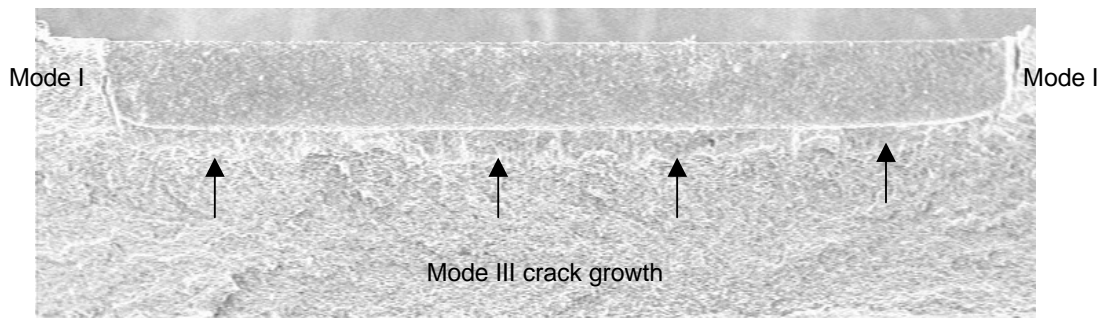


Figure 1. Mode III crack growth through the thickness tube.

Different mixed mode criteria [2-7] have been applied in order to obtain the relationship between crack growth rate and stress intensity factor under multiaxial fatigue. Mixed mode results have been compared with both pure mode I and pure mode II crack growth rates obtained on the same material. None of the applied criteria correctly explains the experimental crack growth rate results.

Regarding the crack path, cracks under mixed mode loading seems to propagate following the direction of the maximum crack propagation rate, as proposed by Hourlier and Pineau [8]. This fact, together with the experimental crack growth rates, explains the failure mechanism of micronotched tubes under torsional fatigue.

EXPERIMENTAL PROCEDURE

Torsional fatigue tests were carried out on tubular specimens with an external diameter of 27.4 mm and a wall thickness ' t ' of 1.3 mm (Figure 2.a.). These specimens came from cold drawn tubes made of 0.35% carbon steel (a SAE1035-like steel). Mechanical properties of the material are: ultimate tensile stress 770 MPa and yield stress 650 MPa. After a hand polishing with emery papers up to #1000 grit. Through-thickness micronotches with a length of 5 mm were then eventually obtained by EDM (electro-discharge machining). In particular, two micronotches directions were used to study a possible effect of anisotropy: longitudinal, along the drawing direction, and transversal, perpendicular to the drawing direction. Figure 2.b.,c. shows the micronotch dimension and directions.

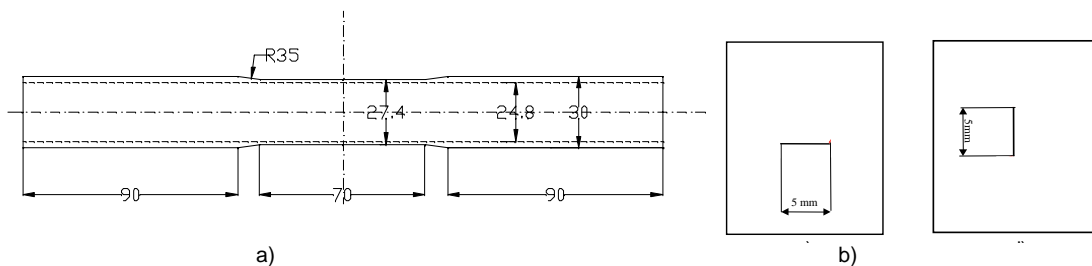


Figure 2. Experimental tests: a) tubular test specimen, b) micronotch directions.

Tests were carried out on a multi-axial MTS 809 testing machine with a torque capacity of 2200 Nm at a frequency of 10 Hz. The crack path and length of the crack during the propagation were monitored by means of plastic replicas.

Specimens were subjected to three different tests: i) mode I propagation tests at $R=-1$ (transverse notch under axial load); ii) mode II propagation (longitudinal notch under torsional load); iii) mixed mode propagation (longitudinal and transverse notch under torsional load) on specimens with mode I branches at the tips of the notches.

RESULTS

Fractographies

Pure mode I and II test were firstly carried out: in particular pure mode II crack propagation have been obtained testing the specimen at alternating torsional test imposing a high torsional stress level.

Figure 3.a. shows the pure mode II crack growth on a vertical notched specimen tested at a high stress level ($\tau_a=150$ MPa, $\Delta K_{II}=18$ MPa \sqrt{m}). Figure 3.b. details the mode II fracture surface.

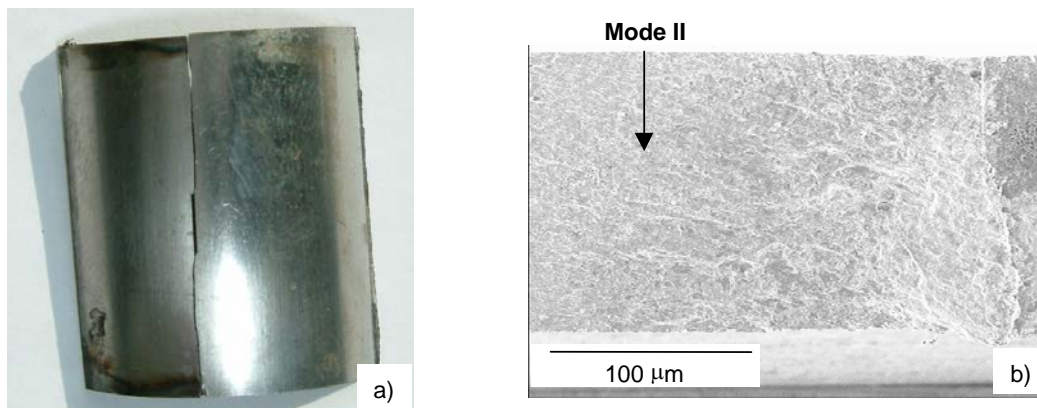


Figure 3. Mode II propagation experiments: a) crack path; b) mode II fracture surface ($\tau_a=150$ MPa, $\Delta K_{II}=18$ MPa \sqrt{m})

The results of pure mode II crack propagation rate are shown in Figure 4, together with the results of pure mode I push-pull test. Mode II crack growth rate results are consistent with the mode III fatigue threshold obtained in [1] - $\Delta K_{III}=9.5$ MPa \sqrt{m} - a value estimated from fatigue limit tests on specimens containing shallow surface longitudinal notches. The mode I fatigue threshold results to be lower than mode II threshold, and the ratio is approx. 1.2.

It is of some importance to remark that the microstructure of the material is constituted by longitudinal ferrite and pearlite elongated grains and that the cracks in mode II are almost parallel to this texture.

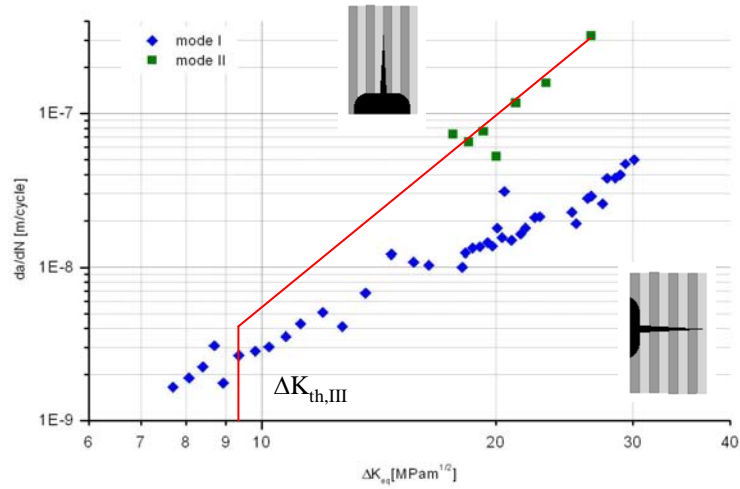


Figure 4. Crack growth experiments at $R=-1$ in mode I and mode II.

A series of torsional tests ($R=-1$) carried out at $\Delta K_{th,III} < \Delta K_{II} < 18 \text{ MPa}\sqrt{\text{m}}$ showed a path characterized by the initial formation of four mode I kinks at the edge of notches and then a subsequent mixed mode propagation along these branches. Figure 5 shows the path of one of the four mixed mode cracks emanating respectively from the transverse notch (Fig. 5.a $\tau_a=127.5 \text{ MPa}$, $\Delta K_{II}=13 \text{ MPa}\sqrt{\text{m}}$) and the vertical notch (Fig. 5.b $\tau_a=100 \text{ MPa}$, $\Delta K_{II}=12 \text{ MPa}\sqrt{\text{m}}$).

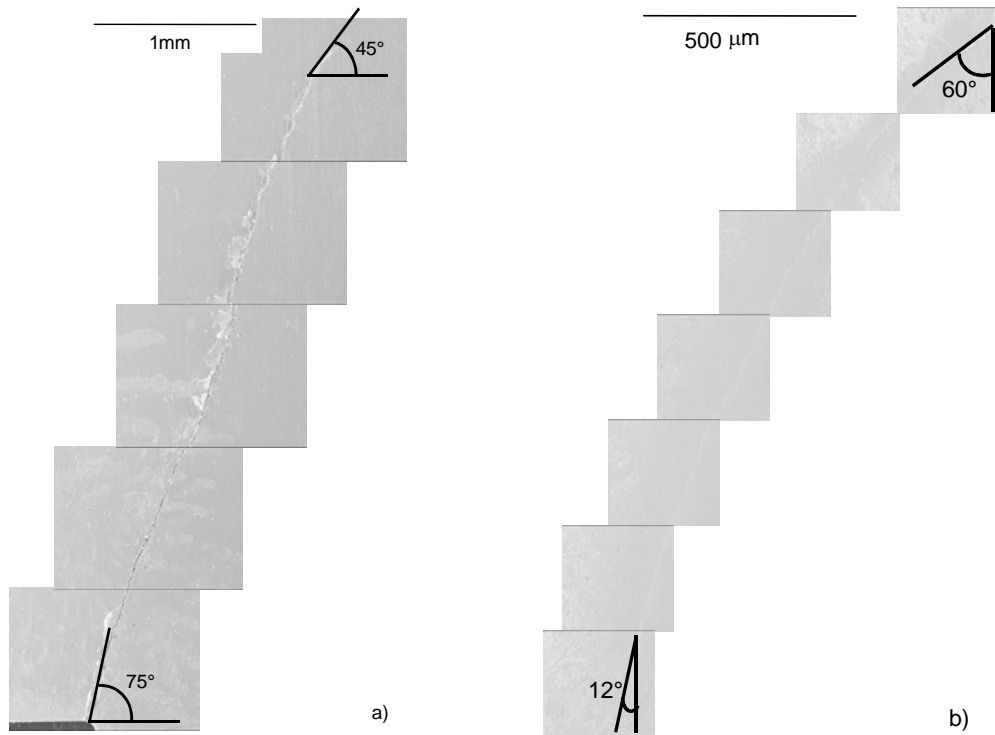


Figure 5. Crack path of mixed mode cracks.

The fractographic observation has revealed in both cases a tortuous path characterized by multiple branched microcracks emanating from the main crack (transverse notch) [3] and a step-wise propagation patterns (vertical notch).

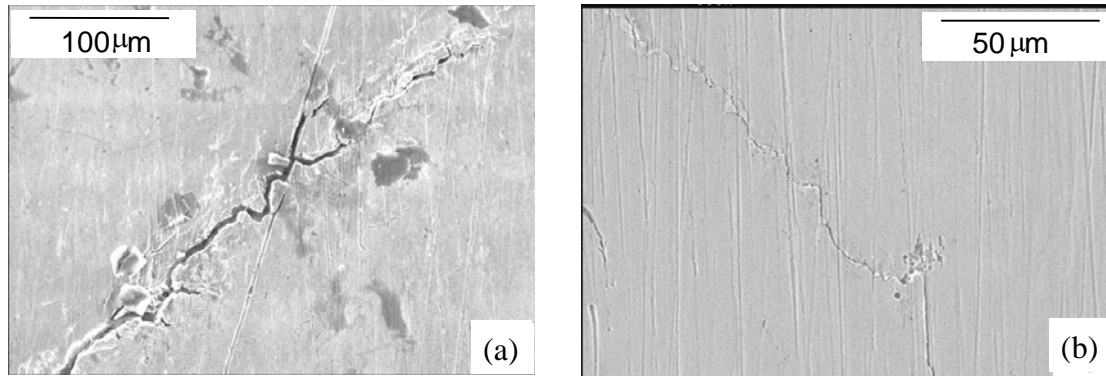


Figure 6. Detail of branched crack propagation: a) transversal notch; b) vertical notch.

FE analysis

In order to determine correctly the SIFs for mode I and mode II along the crack path, a FE analysis of the tubular notched specimen was obtained with a 2D plane-stress model under shear stress. The model has been created with 8-noded ('quadratic') elements. In the FE mesh the different steps, into which the actual crack path was discretized (Figure 7), were considered as linear segments. Figure 8.a. shows the FE crack path of the branched crack emanating from the transversal defect, whereas Figure 8.b represents the path for the vertical notch. The mesh at the crack tips has been refined, the element length being 15 μm. K_I and K_{II} has been calculated by ABAQUS software which derives the SIF's from the J-integral [9].

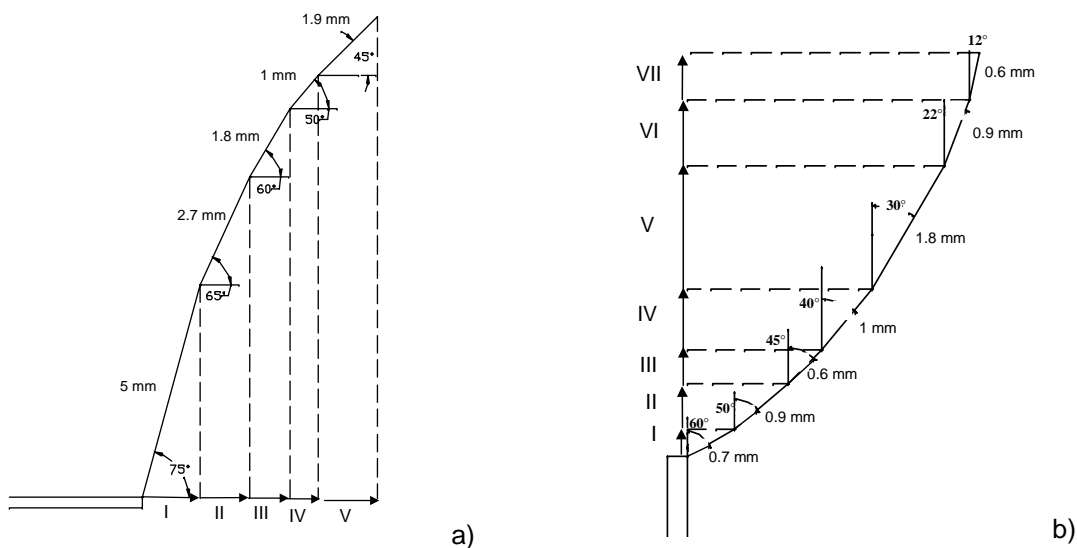


Figure 7. Discretized crack path: a) transverse and b) vertical notch.

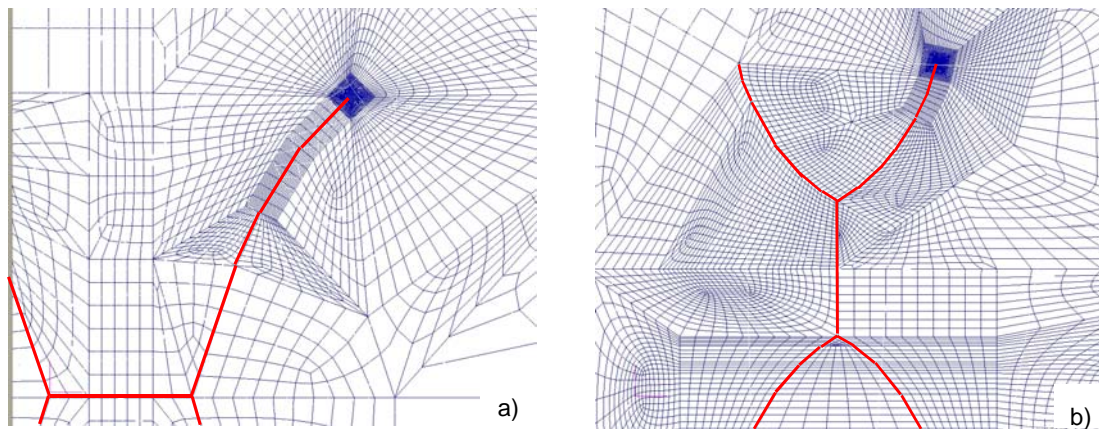


Figure 8. FE model for branched crack: a) transverse notch (V step); b) vertical notch (VII step).

To obtain the effective mode II stress intensity factor, the analysis has been run with a friction coefficient between the crack surfaces of 0.5.

It is of some importance to note that the 4-branches symmetrical fracture pattern induces SIF's that are lower than existing solutions for single branched cracks [10] and a significantly higher mode mixity at the tips of the branches.

Discussion

In the case of mixed mode crack propagation, a first equivalent stress intensity factor was calculated as [11]:

$$\Delta K_{eq} = \sqrt{\Delta K_I^2 + \Delta K_{II}^2} \quad (1)$$

Results are shown in Figure 9: in both cases crack speed in the initial phase is much lower respectively than mode I and mode II propagation.

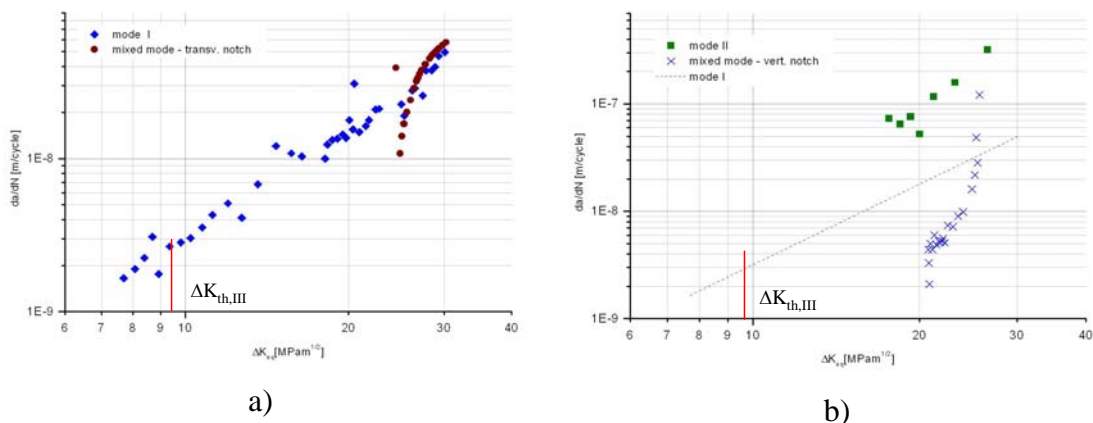


Figure 9. Mixed mode crack growth rate results: a) transversal notch; b) vertical notch.

A more refined analysis has been carried out considering a formulation based onto effective ΔK . In particular in order to take into account crack closure, the effective mode I SIF has been calculated considering only the positive part of the fatigue cycle ($\Delta K_{I,eff}=0.5\cdot\Delta K_I$). Considering an equivalent SIF range defined as [4]:

$$\Delta K_{eq} = \sqrt{\Delta K_{I,eff}^2 + \left[\frac{614}{507} \Delta K_{II,eff}^{3.21} \right]^{2/3.74}} \quad (2)$$

propagation data have been re-analyzed. Results reported in Figure 10 clearly show that, even adopting a different criterion, the propagation rate in mixed mode cannot be analysed in terms of simple ΔK_{eq} concepts.

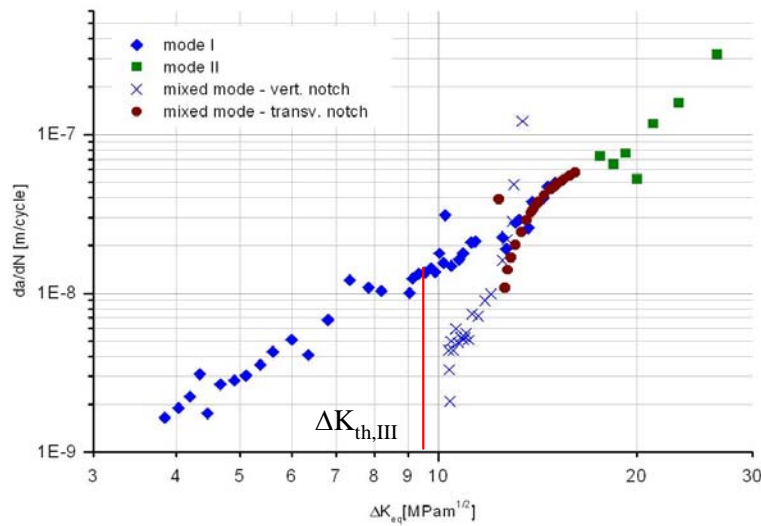


Figure 10. Mixed mode results according to Eq. 2

The results of mixed mode propagation are somehow unexpected since the initial hypothesis for the mode III growth observed in [1] was the anisotropy. However, in spite of the textured material there are not enough evidences for discussing a difference in growth rate caused by anisotropy. Actually, the present results support the findings in [1], since it appears that the preferential mode III coplanar growth at the tip of shallow defects – versus mode I propagation of kinks at defect edges - can be justified in terms of the growth mechanism with higher propagation rate [8].

CONCLUDING REMARKS

A series of mixed mode tests on specimen extracted from a cold drawn tube made of 0.35% carbon steel showed that the crack propagation rate in the initial phase (high

mode mixity) is lower than both pure mode I and mode II crack growth rate while they tend in the final phases to be similar to simple modes. The different applied mixed mode criteria cannot explain in terms of simple ΔK_{eq} this kind of behavior, which is otherwise responsible for stable mode III growth in presence of shallow micronotches in tubular components of the same material.

ACKNOWLEDGEMENTS

This paper has been published under permission of the Tenaris Industrial & Automotive Product Development Division, directed by Dr. Mario A. Rossi, who is kindly acknowledged. The present results have been obtained in the frame of a research contract between Tenaris Dalmine and Politecnico di Milano, Dipartimento di Meccanica.

REFERENCES

1. Beretta S., Cerrini A., Desimone H. (2006), *Mode III threshold for a mild steel in presence of small cracks*, 9th International Fatigue Conference, Atlanta (USA).
2. K. Tanaka, Y. Akiniwa, T. Kato, T. Mikuriya (2004), *Fatigue crack propagation from a precrack under combined torsional and axial loading*, Fatigue Fract Engng Mater Struct, 28, 73-82.
3. S.L. Wong, P.E. Bold, M.W. Brown and R.J. Allen (2000), *Fatigue crack growth rates under sequential mixed mode I and II loading cycles*, Fatigue Fract Engng Mater Struct, 23, 667-674.
4. S. Bogdanski, M.W. Brown (2002), *Modelling the three dimensional behaviour of shallow rolling contact fatigue cracks in rails*, Wear, 253, 17-25.
5. H.A. Richard, M. Fulland, M. Sander (2004), *Theoretical crack path prediction*, Fatigue Fract Engng Mater Struct, 28, 3-12.
6. Pinna C. (1997), *Etude de la propagation des fissures de fatigue sous chargement de cisaillement pla. Application au cas de l'acier maraging M250*, PHD thesis.
7. C. Pinna, V. Doquet (1999), *The preferred fatigue crack propagation mode in a M250 maraging steel loaded in shear*, Fatigue Fract Engng Mater Struct, 22, 173-183.
8. Hourlier F., Pineau A. (1981), *Fatigue crack propagation behavior under complex mode loading*. In: Advances in Fracture Research, Fracture 81 (ICF 5), Vol. 4, pp.1833-1840.
9. ABAQUS 6.4 *User's Manual*, Hibbit Carlson and Sorensens.
10. Y. Murakami et al. (eds.), *Stress intensity factor Handbook*, Pergamon Press, Oxford, 1987.
11. L.P Pook, *Crack Paths*, WIT Press, Southampton, 2002.